Kinesin-3 and dynein mediate microtubule-dependent co-transport of mRNPs and endosomes

Sebastian Baumann[1,2], Thomas Pohlmann[1,2], Marc Jungbluth[2,*], Andreas Brachmann[2,‡] and Michael Feldbrügge[1,2,§]

[1]Heinrich Heine University Düsseldorf, Institute for Microbiology, 40204 Düsseldorf, Germany
[2]Max Planck Institute for Terrestrial Microbiology, Department of Organismic Interactions, Karl-von-Frisch-Str. 10, 35043 Marburg, Germany

*Present address: Philipps University Marburg, Department of Genetics, Karl-von-Frisch-Str. 8, 35043 Marburg, Germany
‡Present address: Biocenter of the Ludwig Maximilians University Munich, Genetics Section, Grosshaderner Str. 2-4, 82152 Planegg-Martinsried, Germany
§Author for correspondence (feldbrue@hhu.de)

Accepted 26 January 2012
Journal of Cell Science 125, 2740–2752

doi: 10.1242/jcs.101212

Summary

Long-distance transport of mRNAs is important in determining polarity in eukaryotes. Molecular motors shuttle large ribonucleoprotein complexes (mRNPs) containing RNA-binding proteins and associated factors along microtubules. However, precise mechanisms including the interplay of molecular motors and a potential connection to membrane trafficking remain elusive. Here, we solve the motor composition of transported mRNPs containing the RNA-binding protein Rrm4 of the pathogen *Ustilago maydis*. The underlying transport process determines the axis of polarity in infectious filaments. Plus-end-directed Kin3, a kinesin-3 type motor, mediates anterograde transport of mRNPs and is also present in transport units moving retrogradely. Split dynein Dyn1–Dyn2 functions in retrograde movement of mRNPs. Plus-end-directed conventional kinesin Kin1 is indirectly involved by transporting minus-end-directed dynein back to plus ends. Importantly, we additionally demonstrate that Rrm4-containing mRNPs colocalise with the t-SNARE Yup1 on shuttling endosomes and that functional endosomes are essential for mRNP movement. Either loss of Kin3 or removal of its lipid-binding pleckstrin-homology domain abolishes Rrm4-dependent movement without preventing colocalisation of Rrm4 and Yup1-positive endosomes. In summary, we uncovered the combination of motors required for mRNP shuttling along microtubules. Furthermore, intimately linked co-transport of endosomes and mRNPs suggests vesicle hitchhiking as mode of mRNP transport.

Key words: RNA recognition motif, Long-distance transport, Vesicle trafficking, *Ustilago maydis*

Introduction

Localised translation in eukaryotes is crucial in determining the subcellular localisation of proteins and thus involved in a number of cellular processes such as establishing and maintaining polarity. An important mechanism is the active transport of mRNAs along the cytoskeleton of actin cables and microtubules for short- and long-distance transport, respectively. Cargo mRNAs are recognised by RNA-binding proteins that associate with accessory factors to form large ribonucleoprotein complexes designated mRNPs (St Johnston, 2005; Holt and Bullock, 2009; Martin and Ephrussi, 2009).

Microtubule-dependent mRNP transport is important for oogenesis, embryogenesis and neuronal processes in higher eukaryotes, as well as for polar growth in fungi (King et al., 2005; Palacios, 2007; Zarnack and Feldbrügge, 2007; Doyle and Kiebler, 2011). Active transport is mediated by unidirectionally moving molecular motors. In most cases, kinesins move cargo towards the plus end of microtubules, whereas their counterpart, dynein, transports cargo towards the minus end (Li and Gundersen, 2008; Gennerich and Vale, 2009).

During oogenesis of *Drosophila melanogaster*, transport and localisation of mRNAs encoding morphogens are essential in determining both main body axes. A well-studied example is the role of Staufen during mRNP trafficking (St Johnston, 2005; Martin and Ephrussi, 2009). This RNA-binding protein is required for *oskar* mRNA localisation and most likely binds stem-loop zip codes in the 3′ UTR (Jenny et al., 2006). mRNPs containing Staufen and *oskar* mRNA that shuttle along microtubules are transported by conventional kinesin predominantly towards the plus ends of microtubules. A biased random walk along a weakly polarised cytoskeleton might result in accumulating *oskar* mRNA at the posterior pole of the oocyte (Zimyanin et al., 2008). During embryogenesis pair-rule transcripts localise to the apical cytoplasm. Here, mRNA zip codes are recognised by the RNA-binding protein egalitarian (Egl), which binds dynein in concert with bicaudal-D (Bic-D) (Dienstbier et al., 2009). It was hypothesised that shuttling mRNPs reach their final destination because the zip-code-mediated coupling of mRNPs to dynein promotes the processivity of the motor complex and thus drives its movement towards microtubule minus ends that are facing to the apical site (Bullock et al., 2006). In addition, dynein plays a part in anchoring mRNPs at the site of their localisation (Delanoue and Davis, 2005; Delanoue et al., 2007).

In *Ustilago maydis*, microtubule-dependent mRNA trafficking is important for pathogenic development (Feldbrügge et al., 2008; Vollmeister and Feldbrügge, 2010). In this pathogen, a morphological switch from yeast-like sporidia to infectious filaments is essential to cause corn smut disease (Kämper et al., 2006; Brefort et al., 2009). The filamentous program is

triggered by a homeodomain transcription factor whose activity is regulated at the level of heterodimerisation (i.e. the formation of a bW–bE heterodimer) (Kämper et al., 1995; Vollmeister et al., 2012). Infectious filaments grow with a defined axis of polarity. They expand at the hyphal tip and insert retraction septa at regular intervals at the basal pole, leading to the formation of characteristic empty sections. Nuclei are positioned in the central regions of filaments (Steinberg et al., 1998). Studies using the microtubule inhibitor benomyl revealed that microtubules are essential for efficient filamentous growth (Fuchs et al., 2005). In the absence of microtubules, filaments are shorter and the formation of retraction septa is impaired. Moreover, the axis of polarity is disturbed as cells initiate bipolar growth (Fuchs et al., 2005). Analysis of microtubule orientation in *U. maydis* filaments revealed that about 90% of microtubules face towards the poles with their plus ends (Schuchardt et al., 2005; Lenz et al., 2006; Schuster et al., 2011b). They serve as tracks for molecular transport units such as endosomes. This was discovered studying the t-SNARE-like protein Yup1 that is involved in the endocytotic uptake of the lipophilic styryl dye FM4-64. Loss-of-function mutants showed a disturbed morphology, which is probably due to alterations in cell wall composition (Wedlich-Söldner et al., 2000). Yup1 and the small GTPase Rab5a colocalise on shuttling endosomes (Fuchs et al., 2006; Schuster et al., 2011a; Schuster et al., 2011b). Their plus-end-directed transport is mediated through Kin3, an UNC-104/KIF1A-like kinesin-3 and the minus-end-directed transport through split dynein Dyn1–Dyn2, whose subunits are encoded by separate genes, *dyn1* and *dyn2* (Straube et al., 2001; Wedlich-Söldner et al., 2002b; Schuster et al., 2011c; Schuster et al., 2011a; Schuster et al., 2011b). This process might mediate the transport of cargo to the basal vacuole for degradation or could promote membrane recycling for a continuous supply of membranes at the apical growth cone (Steinberg, 2007b; Steinberg, 2007a). During sporidial proliferation, shuttling endosomes function in subcellular targeting of small GTPase regulators to septation sites to coordinate cytokinesis and cell separation (Schink and Bölker, 2009).

A second important long-distance transport process is the microtubule-dependent trafficking of mRNAs, which was discovered studying the function of Rrm4 (Vollmeister and Feldbrügge, 2010). Rrm4 is an ELAV-type RNA-binding protein [embryonic lethal abnormal vision, the closest human homologue belongs to the ELAV/HuD family (Becht et al., 2005)]. It contains three N-terminal RNA recognition motifs (RRMs) and a C-terminal MLLE domain [MademoiseLLE, protein–protein interaction domain found at the C terminus of poly(A)-binding protein PABPC (Kozlov et al., 2001; Kozlov et al., 2010)]. Loss of Rrm4 causes aberrant filament formation and reduced pathogenicity (Becht et al., 2005). The protein moves bidirectionally along microtubules in wild-type filaments. Deletion of *kin1*, which encodes conventional kinesin (Lehmler et al., 1997) results in an accumulation of Rrm4 at the poles (Becht et al., 2006). This accumulation at the microtubule plus ends is probably an indirect effect, because Kin1 recycles dynein to maintain a constant reservoir of accessible dynein at the plus ends (Lenz et al., 2006). A combination of in vivo UV crosslinking and RNA live imaging demonstrated that Rrm4 recognises and transports a distinct set of mRNAs encoding, for example, translation and polarity factors (König et al., 2009). Consistently, the poly(A)-binding protein Pab1, which associates with the poly(A) tail of most eukaryotic mRNAs (Hogan et al., 2008), colocalises with Rrm4 in shuttling particles. In the absence of Rrm4, Pab1 is no longer transported, indicating that Rrm4 is part of the primary transport unit and functions as the key RNA-binding protein during mRNA transport (König et al., 2009). Its target mRNAs contain potentially CA-rich binding sites that function as RNA zip codes to promote frequency and processivity of microtubule-dependent transport (König et al., 2009). Removal of the three RRMs of Rrm4 results in a non-functional protein that still shuttles along microtubules. However, microtubule-dependent transport of target mRNA is hampered. Consequently, filaments grow similar to the *rrm4Δ* strain, exhibiting impaired formation of retraction septa and altered polarity. Thus, the RNA-binding domain is functionally important, and Rrm4 does not hitchhike on transported mRNAs, but is an integral part of the transport unit (König et al., 2009). According to current views, microtubule-dependent transport of mRNPs is important for determination of the subcellular localisation of targets such as the small G protein Rho3 at retraction septa, as well as crucial for efficient secretion of the endochitinase Cts1 (König et al., 2009; Zarnack and Feldbrügge, 2010; Koepke et al., 2011).

Results

Loss of Kin1 causes accumulation of mRNPs at both poles of mutant filaments

To investigate the involvement of Kin1 in mRNP transport, we analysed the subcellular localisation of Rrm4 and Pab1 in filaments in the absence of Kin1. Studies were performed using strain AB33 expressing an active bW2–bE1 heterodimeric transcription factor controlled by the nitrate-inducible *nar1* promoter (Table 1). Thus, changing the nitrogen source of the medium activates bW2–bE1 expression and subsequent formation of an active heterodimer. This is sufficient to trigger filamentous growth synchronously and highly reproducibly (Brachmann et al., 2001).

As previously shown (König et al., 2009), Rrm4G and Pab1R (functional C-terminal fusion proteins of Rrm4 and Pab1 with the enhanced version of the green fluorescence protein eGFP and the monomeric red fluorescence protein mRFP, respectively) colocalised in mRNPs that were transported along microtubules (supplementary material Fig. S1A, Movie 1). Rrm4G$^{RRM\Delta}$ lacking all three RRMs also shuttled along microtubules, even though mRNA transport was lost. Consequently, the respective strains showed the loss-of-function phenotype (supplementary material Fig. S1B) (König et al., 2009). Here, we show that Pab1R was no longer part of the transport units in this strain (supplementary material Fig. S1B, Movie 2). This is consistent with earlier results investigating the transport of *ubi1* mRNA by RNA live imaging (König et al., 2009). We observed a high concentration of Pab1R in the initial cell with decreasing intensity towards both poles (supplementary material Fig. S1B). This is reminiscent of the Pab1 gradient observed in *rrm4Δ* filaments, suggesting a disturbed mRNA distribution (König et al., 2009). Thus, Rrm4 can be considered as an integral part of the transport unit, whereas Pab1 serves as a molecular marker for the presence of transported mRNAs. The presence of both proteins is an indicator of intact mRNPs (König et al., 2009; Zarnack and Feldbrügge, 2010).

The mRNP markers were used to investigate the role of conventional kinesin Kin1 by deleting *kin1* in AB33rrm4G/

Table 1. *U. maydis* strains used in this study

Strain	Locus	Progenitor	Specific comment	Reference
FB1			Wild type, mating type *a1b1*	(Banuett and Herskowitz, 1989)
FB2			Wild type, mating type *a2b2*	(Banuett and Herskowitz, 1989)
UM521			Wild type, mating type *a1b1*, genome sequenced	(Kämper et al., 2006)
AB33	*b*	FB2	P_{nar}*:bW2bE1*, expression of active b heterodimer under control of the *nar1* promoter, strain grows filamentously upon changing the nitrogen source	(Wedlich-Söldner et al., 2002)
AB5	*b*	FB1	P_{nar}*:bW2bE1*, comparable to AB33 but in the genetic background of FB1	This study
AB5dyn2^{ts}	*dyn2*	AB5	Carrying a temperature sensitive allele of *dyn2*	(Wedlich-Söldner et al., 2002)
AB5dyn2^{ts}/rrm4G	*dyn2* *rrm4*	AB5dyn2^{ts}	Expressing Rrm4 fused to enhanced version of eGFP	This study
AB5dyn2^{ts}/rrm4G/ pab1R	*dyn2* *rrm4* *pab1*	AB5dyn2^{ts}/rrm4G	Expressing Pab1 fused to monomeric version of RFP	This study
AB33rrm4G	*rrm4*	AB33	Expressing Rrm4 fused to eGFP	(Becht et al., 2006)
AB33rrm4G/pab1R	*rrm4* *pab1*	AB33rrm4G	Expressing Pab1 fused to mRFP	(König et al., 2009)
AB33rrm4G$^{RRM\Delta}$/ pab1R	*rrm4* *pab1*	AB33pab1R/ rrm4G	Expressing Rrm4 without RRMs fused to eGFP	This study
AB33rrm4G/kin1Δ	*rrm4* *kin1*	AB33rrm4G	Carrying a deletion in *kin1*	(Becht et al., 2006)
AB33rrm4G/pab1R/ kin1Δ	*rrm4* *pab1* *kin1*	AB33pab1R/ rrm4G	Carrying a deletion in *kin1*	This study
AB33rrm4G$^{RRM\Delta}$/ pab1R/kin1Δ	*rrm4* *pab1* *kin1*	AB33rrm4G$^{RRM\Delta}$/ pab1R	Expressing Rrm4 version without RRMs fused to eGFP and carrying a deletion in *kin1*	This study
AB33rrm4R/dyn2G^{3}	*rrm4* *dyn2*	AB33rrm4R	Expressing Dyn2 fused at the C-terminus to triple eGFP	This study
AB33rrm4G/kin3Δ	*rrm4* *kin3*	AB33rrm4G	Carrying a deletion in *kin3*	This study
AB33rrm4G/pab1R/ kin3Δ	*rrm4* *pab1* *kin3*	AB33pab1R/ rrm4G	Carrying a deletion in *kin3*	This study
AB33kin3G^{3}	*kin3*	AB33	Expressing Kin3 fused at the C-terminus to triple eGFP	This study
AB33rrm4R/kin3G^{3}	*rrm4* *kin3*	AB33rrm4R	Expressing Kin3 fused at the C-terminus to triple eGFP	This study
AB33rrm4G/P$_{otef}$yup1C	*rrm4* *ip^{s}*	AB33rrm4G	Expressing Yup1 fused to mCherry under control of the constitutively active promoter P$_{otef}$; defined ectopic integration at the *ip^{s}* locus, encoding a carboxin-sensitive iron sulfur protein	(Loubradou et al., 2001; Wedlich-Söldner et al., 2000)
AB33rrm4Δ/P$_{otef}$yup1C	*rrm4* *ip^{s}*	AB33rrm4G	Carrying a deletion in *rrm4*	This study
AB33rrm4R/kin3Δ	*rrm4* *kin3*	AB33rrm4R	Carrying a deletion in *kin3*	This study
AB33rrm4R/kin3$^{PH\Delta}$G^{3}	*rrm4* *kin3*	AB33rrm4R/ kin3Δ	Expressing Kin3 version without pleckstrin-homology domain and fused at the C-terminus to triple eGFP	This study
AB33rrm4GT/ P$_{otef}$yup1CM	*rrm4* *ip^{s}*	AB33rrm4GT	Expressing Rrm4 with tandem affinity protein tag fused to eGFP and Yup1 fused to mCherry containing a triple Myc epitope tag	This study
AB33rrm4GT/ P$_{otef}$yup1CM/ kin3$^{PH\Delta}$−HA^{3}	*rrm4* *ip^{s}* *kin3*	AB33rrm4GT/ P$_{otef}$yup1CM	Expressing Kin3 version without pleckstrin-homology domain and fused at the C-terminus to triple HA epitope	This study
AB33rrm4GT/ P$_{otef}$yup1CM/kin3Δ	*rrm4* *ip^{s}* *kin3*	AB33rrm4GT/ P$_{otef}$yup1CM	Carrying a deletion in *kin3*	This study
AB33yup1^{ts}	*yup1*	AB33	Carrying a temperature sensitive allele of *yup1*	(G. Steinberg, unpublished)
AB33yup1^{ts}/rrm4G	*yup1* *rrm4*	AB33yup1^{ts}	Expressing Rrm4 fused to eGFP	This study
AB33yup1^{ts}/rrm4G/ P$_{otef}$yup1C	*yup1* *rrm4*	AB33yup1^{ts}/ rrm4G	Expressing Yup1–mCherry under control of the constitutively active promoter P$_{otef}$ to complement the mutant; defined ectopic integration at the *ip^{s}* locus	(Loubradou et al., 2001; Wedlich-Söldner et al., 2000)
AB33P$_{otef}$rab5aG	*ip^{s}*	AB33	Expressing eGFP-Rab5a ectopically under control of the constitutively active promoter P$_{otef}$ at the *ip^{s}* locus	This study
AB33yup1^{ts}/ P$_{otef}$rab5aG	*rab5a* *yup1* *ip^{s}*	AB33yup1^{ts}	Expressing eGFP-Rab5a ectopically under control of the promoter P$_{otef}$ at the *ip^{s}* locus; temperature-sensitive allele of *yup1*	This study

pab1R. As shown previously (Becht et al., 2006), loss of Kin1 led to defects in filamentous growth that resembled those of *rrm4Δ* strains (supplementary material Fig. S1C). In accordance with the observation that Kin1 transports split dynein Dyn1–Dyn2 to the plus ends of microtubules at hyphal tips (Lenz et al., 2006), movement of Rrm4G was drastically reduced and the protein accumulated at both poles of the aberrantly growing filaments (supplementary material Fig. S1C) (Becht et al., 2006). Here, we demonstrate that distribution of Pab1R was also disturbed because a gradient of Pab1R emanated from the filament centre. In addition, Pab1R colocalised with Rrm4G at the hyphal poles, indicating an accumulation of mRNPs at these sites (48 of 49 polar Rrm4G accumulations in 26 filaments also showed Pab1R accumulation; supplementary material Fig. S1C). Residual moving units contained both Rrm4G and Pab1R (supplementary material Movie 3). In strains expressing $Rrm4G^{RRM\Delta}$, Pab1 no longer accumulated at the poles (none of the 40 polar Rrm4 accumulations in 24 filaments colocalised with Pab1R; supplementary material Fig. S1D), demonstrating that $Rrm4G^{RRM\Delta}$ particles were devoid of mRNA. These observations confirmed that Rrm4G movement is independent of the presence of mRNA in the particles whereas Pab1R hitchhikes on transported mRNAs and can thus serve as an in vivo marker for mRNP transport. Taking advantage of these markers, we showed that conventional kinesin is involved in the transport of mRNPs containing Rrm4 and Pab1. As previously suggested, this influence is indirect, because Kin1 is essential for the accumulation of Dyn1–Dyn2 at the plus ends of microtubules, forming a potential dynein-loading zone (Lenz et al., 2006; Schuster et al., 2011c).

Dyn2 is necessary for mRNP shuttling and colocalises with Rrm4 in vivo

The observed role of Kin1 during mRNA transport suggested that split dynein Dyn1–Dyn2 mediates retrograde transport of mRNPs (Lenz et al., 2006). To test this hypothesis, we made use of a temperature-sensitive allele of *dyn2* that causes inactivation of dynein at restrictive temperatures (Wedlich-Söldner et al., 2002a) (Table 1). The allele was originally identified in the genetic background of strain FB1 (mating type *a1b1*). So far, it has been impossible to generate viable transformants carrying the $dyn2^{ts}$ allele at the homologous locus of FB2 (mating type *a2b2*) or its derivative AB33, suggesting that its temperature sensitivity is closely linked to the genetic background of FB1 (Table 1). Therefore, we used strain AB5 carrying an active bW2–bE1 heterodimeric transcription factor under control of the *nar1* promoter in the genetic background of FB1, which tolerated integration of the temperature-sensitive allele (see the Materials and Methods; Table 1). As in AB33, filamentous growth can be elicited in AB5 by changing the nitrogen source of the medium (see above). To examine mRNP movement in the absence of functional Dyn2 we generated the marker strain $AB5dyn2^{ts}$/rrm4G/pab1R. Growth assays with yeast-like cells verified that $dyn2^{ts}$-carrying strains were viable at permissive temperatures, but failed to grow under restrictive conditions (Fig. 1A). Under filament-inducing conditions at permissive temperatures, the vast majority of filaments grew unipolar, and shuttling of Rrm4G- and Pab1R-containing mRNPs was comparable to that in the wild type (supplementary material Movie 4; Fig. 1B,D). Occasionally, mRNPs accumulated within the cytoplasm indicating that the temperature-sensitive motor exhibited minor transport defects

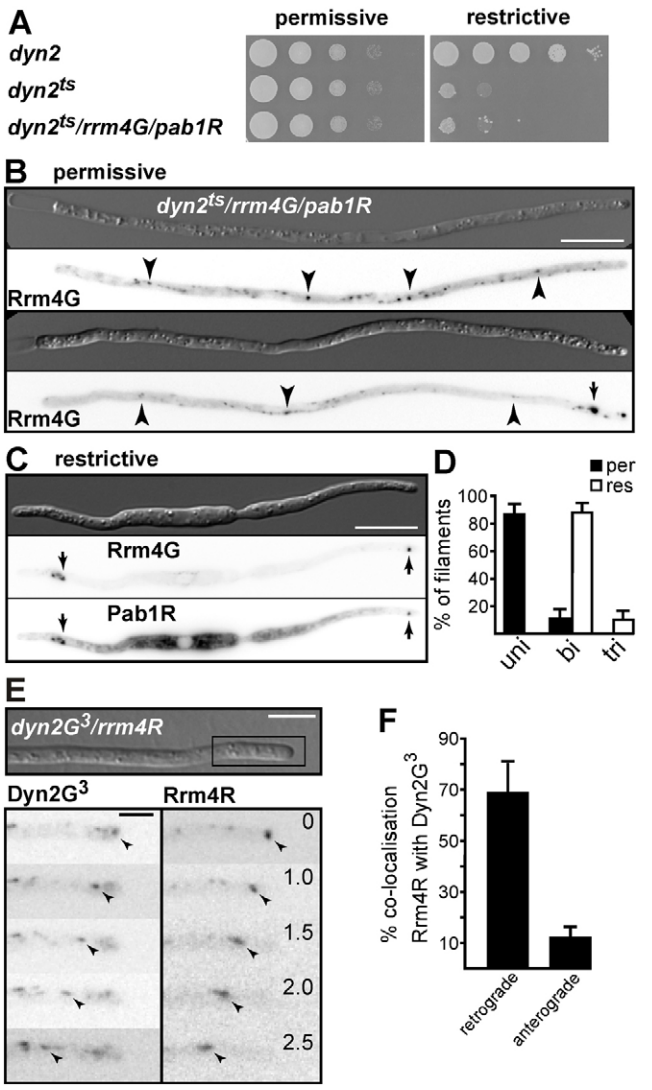

Fig. 1. Dyn2 is essential for Rrm4 transport and colocalises with Rrm4-containing units. (**A**) Growth of AB5 and derivatives carrying a temperature-sensitive mutation in *dyn2*. Plates were incubated at permissive or restrictive temperatures. (**B**,**C**) Filaments of $AB5dyn2^{ts}$/rrm4G/pab1R at permissive (B, two Rrm4G examples) and restrictive (C) temperatures. Filamentous growth was elicited by changing the nitrogen source of the medium resulting in transcriptional activation of the bW2–bE1 heterodimer (see text for details). Arrowheads and arrows indicate moving particles and large immobile accumulations, respectively (see supplementary material Movies 4, 5). Scale bars: 10 µm. (**D**) Bar diagram showing percentage of filaments that grow unipolarly (uni), bipolarly (bi) and tripolarly (tri) at permissive (per) and restrictive (res) temperatures (error bars, s.e.m.). (**E**) Filaments of $AB33dyn2G^3$/rrm4R. Rectangle indicates region magnified below. Inverted frames are taken from supplementary material Movie 6 recorded with dual-colour detection. RFP and GFP images recorded simultaneously are shown juxtaposed. Scale bars: 5 µm (top) and 2.5 µm (bottom). The elapsed time is given in seconds. (**F**) Bar diagram showing the percentage of mobile Rrm4R signals that colocalise with $Dyn2G^3$ in the retrograde and anterograde direction (error bars, s.e.m.).

(Fig. 1B, lower panel). At restrictive temperatures, however, 89% of filaments grew bipolar and 11% even tripolar, indicating that minus-end-directed transport is essential in determining the axis of polarity in b-dependent infectious filaments (Fig. 1C,D).

Importantly, mRNPs containing Rrm4G and Pab1R accumulated at the plus ends of microtubules at both poles (Fig. 1C; 24 filaments with 42 Rrm4G accumulations, 100% colocalisation with Pab1R accumulations; supplementary material Movie 5). In addition, a Pab1R gradient was observed emanating from the filament centre, indicating disturbed mRNA distribution. No residual movement of mRNPs could be detected. Consequently, the split dynein subunit Dyn2 is essential for the transport of Rrm4-containing mRNPs.

To verify whether Rrm4-containing mRNPs are still transported towards the poles in the absence of functional Dyn2, we analysed strain AB5dyn2^{ts}/rrm4G at permissive temperature and shortly after shifting to the restrictive temperature (supplementary material Fig. S2). The number of shuttling Rrm4G-containing units was drastically reduced at the restrictive temperature. However, most of the remaining Rrm4G signals moved processively towards the poles, suggesting that Rrm4 reaches the poles at least in part by plus-end-directed movement along microtubules. Interestingly, during this process Rrm4 pauses for a brief amount of time, and instead of reversing it, continues movement towards the plus ends (supplementary material Fig. S2). Apparently, in the absence of the minus-end-directed motor, reverting to retrograde movement is impossible.

To analyse colocalisation in vivo, we generated strain AB33dyn2G^3/rrm4R, which expresses the functional fusion proteins of Dyn2 and Rrm4 fused C-terminally to triple GFP and mRFP, respectively (Becht et al., 2006; Lenz et al., 2006). Upon filament induction, Dyn2G^3 and Rrm4R colocalised in shuttling units, suggesting that dynein is involved in transporting Rrm4-containing mRNPs (Fig. 1E; supplementary material Movies 6, 7). Because polarisation of the microtubule cytoskeleton is highest at the poles, where about 90% of plus ends face towards filament tips (Schuchardt et al., 2005; Lenz et al., 2006), we quantified the colocalisation of Rrm4-containing mRNPs with Dyn2G^3 in the hyphal apex (three independent experiments, ten filaments per experiment, zone of measurement 10 µm from the tip, 62 and 80 Rrm4R signals moving anterogradely and retrogradely, respectively). A total of 12% of anterogradely and 69% of retrogradely moving Rrm4R signals colocalised with Dyn2G^3 (Fig. 1F), indicating that Dyn2G^3 is mainly associated with minus-end-directed Rrm4R particles. As Dyn2G^3 signals were close to the detection limit, a higher degree of colocalisation cannot be expected with our experimental set-up (supplementary material Movies 6, 7). Thus, the involvement of additional motors for retrograde movement appears unlikely. Taken together, our experiments demonstrate that split dynein mediates retrograde transport of Rrm4-containing mRNPs.

Kin3 is necessary for mRNP shuttling and colocalises with Rrm4 in vivo

Kin1 plays only an indirect role in Rrm4 transport. Hence, the motor mediating plus-end-directed movement of mRNPs is still unknown. At present, only Kin1 and Kin3 have been described to exhibit defects in filamentous growth (Schuchardt et al., 2005). Therefore, we deleted *kin3* in the marker strain AB33rrm4G/pab1R (Table 1). The vast majority of respective filaments grew with a disturbed axis of polarity, and the insertion of retraction septa was impaired (Fig. 2A,B) (Schuchardt et al., 2005). Rrm4G and Pab1R mainly colocalised in large immobile accumulations in the initial cell (Fig. 2A; supplementary material Movie 8). These accumulations resembled the localisation of cytoplasmic and perinuclear microtubule-organising centres, indicating that in the absence of Kin3, mRNPs are trapped at the minus ends of microtubules (Straube et al., 2003; Lenz et al., 2006). The

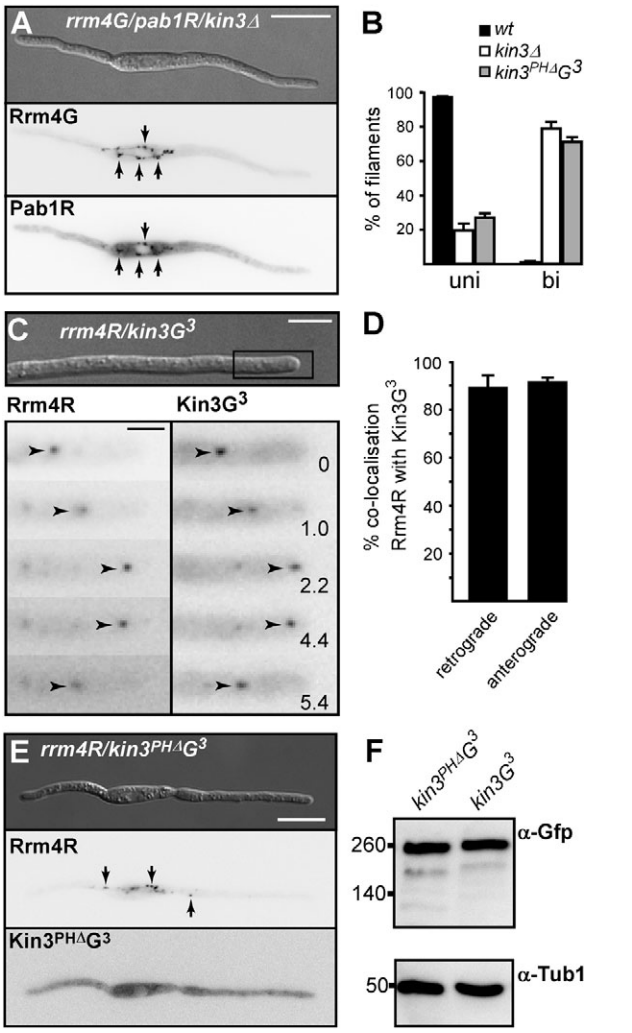

Fig. 2. Kin3 is essential for mRNP transport and colocalises with Rrm4 in shuttling mRNPs. (**A**) RFP and GFP images of AB33rrm4G/pab1R/kin3Δ filament recorded simultaneously are shown juxtaposed (supplementary material Movie 8). Filamentous growth was elicited by changing the nitrogen source of the medium resulting in transcriptional activation of the bW2–bE1 heterodimer (see text for details). Arrows indicate larger immobile accumulations. Scale bar: 10 µm. (**B**) Bar diagram showing percentage of filaments that grow unipolarly (uni) and bipolarly (bi; error bars, s.e.m.; wt, *kin3Δ* and *kin3^{PHΔ}G^3* correspond to strains AB33rrm4G/pab1R, AB33rrm4G/pab1R/kin3Δ and AB33rrm4R/kin3^{PHΔ}G^3, respectively). (**C**) Filament of AB33rrm4R/kin3G^3. Rectangle indicates region that is magnified below. Arrowheads indicate moving particles. Inverted frames are taken from supplementary material Movie 9 recorded with dual-colour detection. RFP and GFP images recorded simultaneously are shown juxtaposed. Scale bars: 5 µm (top) and 2 µm (bottom). Elapsed time is given in seconds. (**D**) Bar diagram showing the percentage of mobile Rrm4R signals that colocalise with Kin3G^3 in the anterograde and retrograde direction (error bars, s.e.m.). (**E**) Filament of AB33rrm4R/kin3^{PHΔ}G^3. Inverted frames are taken from supplementary material Movie 11 recorded with dual-colour detection. RFP and GFP images recorded simultaneously are shown juxtaposed. Arrows indicate larger immobile accumulations. Scale bar: 10 µm. (**F**) Western blot detecting Kin3 variants fused to triple GFP (indicated above the lanes). Antibodies used are given on the right (marker in kDa). Detection of tubulin (Tub1) serves as a loading control.

amount of Rrm4-containing units was reduced about threefold compared with the control strain that has functional Kin3 (three independent experiments, ten filaments per experiment, average Rrm4G signals 55±1.7 and 20±1.1 in AB33rrm4G/pab1R and AB33rrm4G/pab1R/kin3Δ, respectively), which is probably due to an accumulation of Rrm4G particles so that fewer signals can be resolved. Importantly, there was hardly any residual movement detectable, suggesting that Kin3 is exclusively responsible for anterograde transport.

To test colocalisation of Rrm4 and the anterograde motor, we generated strain AB33rrm4R/kin3G^3. Rrm4R and Kin3G^3 colocalised in shuttling particles throughout the filament (Fig. 2C; supplementary material Movies 9, 10). Particles moved with comparable frequency in both directions, suggesting that the plus-end-directed Kin3 does not dissociate from the transport complex during retrograde motion (Fig. 2D; 92% in anterograde and 90% in retrograde direction; three independent experiments, eight to ten filaments per experiment, zone of measurement 10 μm from the tip, 49 and 53 Rrm4R signals moving anterogradely and retrogradely, respectively).

Kin3 contains a conserved pleckstrin homology (PH) domain at its C terminus (position 1570–1670 of 1676 amino acids; SMART accession SM00233, E-value 1.69e^{-11}) (Letunic et al., 2009). For UNC-104, it was shown that this evolutionarily conserved domain interacts specifically with phosphatidylinositol-4,5-bisphosphate and is necessary for vesicle transport in nematodes (Klopfenstein et al., 2002; Klopfenstein and Vale, 2004). To address whether this domain of Kin3 is important for mRNP transport in *U. maydis*, we generated the strain AB33rrm4R/kin3$^{PH\Delta}$G^3 expressing a Kin3G^3 variant lacking the PH domain. The respective strain exhibited a growth phenotype comparable to *kin3Δ* mutants, with the vast majority of filaments growing bipolar (Fig. 2B,E). This suggests that Kin3$^{PH\Delta}$G^3 is non-functional. Consistently, fluorescence microscopy revealed that Rrm4R accumulated in large immobile units in the central region of mutant filaments (Fig. 2E; supplementary material Movie 11), which is reminiscent of the results obtained for *kin3Δ* strains (Fig. 2A). Analysis of the subcellular localisation of Kin3$^{PH\Delta}$G^3 revealed no accumulations, but rather a dispersed distribution throughout the cytoplasm, indicating that the specific localisation to shuttling units was lost (Fig. 2E; supplementary material Movie 11). This was not due to altered expression or protein stability, because western blot experiments verified that the mutation does not cause drastic changes in protein amounts (Fig. 2F). In summary, Kin3 mediates anterograde transport of Rrm4-containing mRNPs and the vesicle-binding domain of Kin3 is essential for this transport process.

Rrm4 colocalises with FM4-64-positive endosomes

The lipid-binding PH domain of kinesin-3 type motors is crucial for endosomal transport (Klopfenstein and Vale, 2004), and the same set of motors is used for the transport of endosomes and mRNPs in filaments of *U. maydis* (Wedlich-Söldner et al., 2002b; Schuster et al., 2011a). This suggests that endosomes and mRNPs share their transport system. To validate this assumption, we stained filaments with the styryl dye FM4-64. This dye labels membranes and enters eukaryotic cells by endocytosis. Thus, it initially stains the plasma membrane, then the vesicles classified as early endosomes, and finally, the vacuole (Vida and Emr, 1995; Wedlich-Söldner et al., 2000). Staining of AB33kin3G^3 revealed that Kin3G^3 colocalised with FM4-64-labelled vesicles that shuttle throughout the filament (Fig. 3A) consistent with previous results demonstrating that Kin3 is the plus-end-directed motor for endosome transport (Wedlich-Söldner et al., 2002b; Schuster et al., 2011a; Schuster et al., 2011b).

Importantly, staining of AB33rrm4G with FM4-64 revealed that Rrm4G also colocalises with these shuttling endosomes (Fig. 3B). To further substantiate our finding that Rrm4G colocalises with FM4-64-positive endosomes, we subjected strains with impaired functions in microtubule-dependent motors to FM4-64 staining. In filaments of AB33rrm4G/kin1Δ or AB5rrm4G/dyn2^{ts}, staining at the restrictive temperature revealed colocalisation of Rrm4G and FM4-64 at the growing poles, suggesting that neither Kin1 nor active split Dyn1–Dyn2 is essential for colocalisation (Fig. 3C,D). Filaments of stained AB33rrm4G/kin3Δ showed that Rrm4G and FM4-64 colocalise in the centre of the initial cell, suggesting that the presence of Kin3 is also not crucial for colocalisation (Fig. 3E). In essence, Rrm4G colocalises with FM4-64-positive endosomes in vivo and Kin1, active split Dyn1–Dyn2 or Kin3 are dispensable for this colocalisation.

Shuttling Rrm4 particles are present almost exclusively on Yup1-positive endosomes

The t-SNARE Yup1 is a characteristic marker for FM4-64-positives endosomes that shuttle bidirectionally along microtubules and are transported by Kin3 and Dyn1–Dyn2 (Wedlich-Söldner et al., 2000; Wedlich-Söldner et al., 2002b; Schuster et al., 2011a). For verification and quantification of the important finding that Rrm4 and endosomes colocalise and are co-transported along microtubules, we generated strain AB33rrm4G/P$_{otef}$yup1C expressing a C-terminal fusion of Yup1 with mCherry (a derivative of mRFP) (Shaner et al., 2004) under control of the constitutively active promoter P$_{otef}$ (Brachmann et al., 2004). The corresponding construct was targeted to the *ip^S* locus, resulting in the high expression of Yup1C in addition to the wild-type protein (see Materials and Methods; Table 1). This results in strong signals without interfering with cell morphology (Wedlich-Söldner et al., 2000).

The vast majority of shuttling Rrm4G colocalised with Yup1C on endosomes throughout the filament (Fig. 4A; supplementary material Movies 12, 13). Quantification of the colocalisation in the hyphal tip region revealed that 89% and 88% of anterogradely and retrogradely moving Rrm4G signals, respectively, coincided with moving Yup1C (three independent experiments, five filaments per experiment, zone of measurement 10 μm from the tip, 67 and 71 Rrm4 signals moving anterogradely and retrogradely, respectively, Fig. 4B).

Because Kin3 colocalised with Rrm4 in the same unit shuttling in both directions (Fig. 2C,D), we investigated whether colocalisation of Rrm4 and Yup1-positive endosomes was dependent on Kin3. To this end, we generated the strains AB33rrm4GT/yup1CM/kin3Δ and AB33rrm4GT/yup1CM/kin3$^{PH\Delta}$HA both expressing two functional fusion proteins: Rrm4 fused to eGFP and a tandem affinity tag, as well as Yup1 fused to mCherry and a triple Myc epitope tag (König et al., 2009). The first strain carried a deletion in *kin3* and the second expressed Kin3 lacking its PH domain fused to a triple HA epitope tag [influenza hemagglutinin peptide, (Niman et al., 1983); (Table 1)]. Investigation of the corresponding filaments revealed that, in both cases, Rrm4GT and Yup1CM colocalised in accumulations at the centre of the initial cell, indicating that Kin3 as well as its lipid-binding domain were dispensable for the

colocalisation of Rrm4- and Yup1-positive endosomes. In summary, Rrm4-containing mRNPs almost always travel in concert with Yup1-positive endosomes and their colocalisation is independent of Kin3.

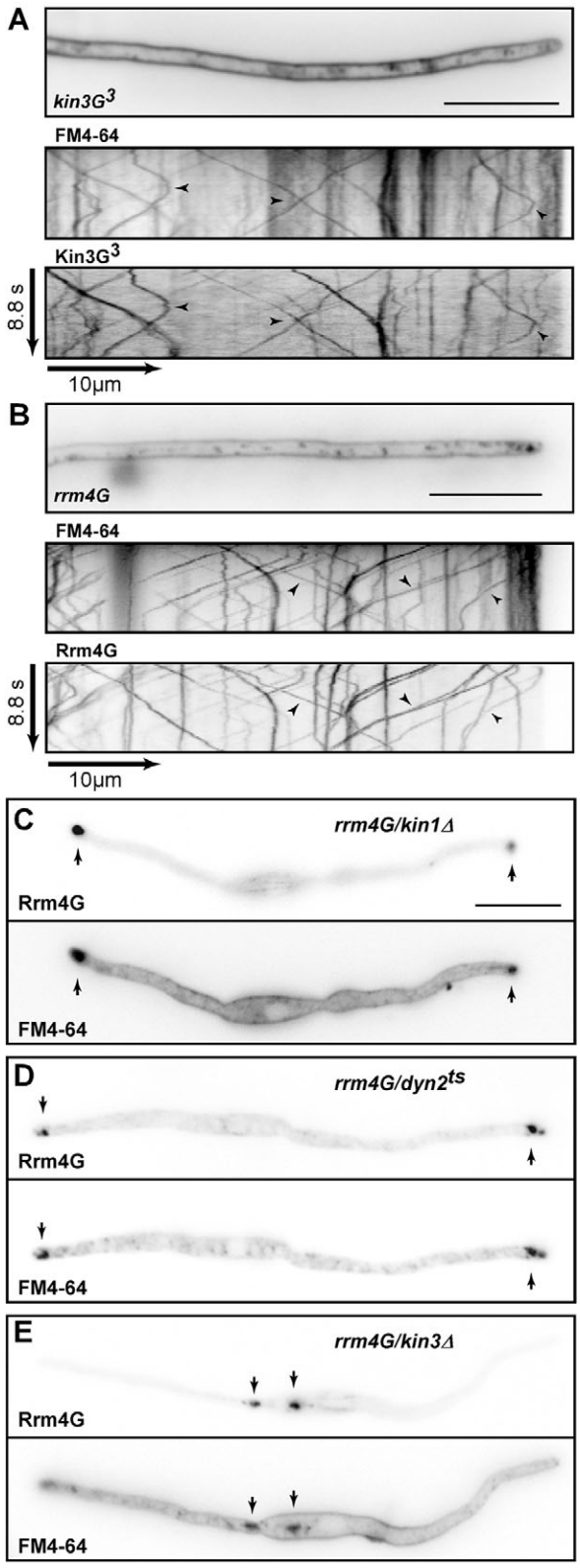

Functional Yup1- and Rab5a-positive endosomes are essential for Rrm4 transport

To investigate whether Rrm4 influences endosome movement, we generated strain AB33P_{otef}yup1C/rrm4Δ. Analysis of this strain in comparison to the control strain expressing Rrm4G and Yup1C revealed that shuttling of Yup1C-containing endosomes was not changed in the absence of Rrm4. This indicates that lack of mRNPs does not impair long-distance movement of endosomes (Fig. 5A). To study their reciprocal relationship, that is whether functional Yup1-positive vesicles are needed for Rrm4 transport, we used a temperature-sensitive mutant of *yup1*. We introduced *rrm4G* in the genetic background of AB33yup1^{ts} (G. Steinberg, unpublished) carrying the temperature sensitive allele of *yup1*^{ts} (Wedlich-Söldner et al., 2000) at the homologous locus. Growth assays verified that *yup1*^{ts}-carrying strains grew filamentously at the permissive temperature, but failed to form filaments under restrictive conditions (supplementary material Fig. S3). Mutant growth under restrictive conditions could be complemented by expressing Yup1C under control of the constitutively active P_{otef} promoter at the *ip*^{S} locus (supplementary material Fig. S3; Table 1).

Fluorescence microscopy of AB33yup1^{ts}/rrm4G filaments under permissive conditions revealed that Rrm4G moved bidirectionally along microtubules in a manner comparable to Rrm4G of the control strain AB33rrm4G/pab1R (Fig. 5B, restrictive temperature at time point t_0). However, after prolonged growth at the restrictive temperature, Rrm4G movement was affected, and after 60 minutes, processive movement of Rrm4G could hardly be observed (Fig. 5B, kymograph lower right panel at t_3). To address whether this altered movement of Rrm4 is due to the detachment of mRNPs and endosomes, we investigated the loss of Yup1 during filamentous growth in closer detail. To check whether endosomes disintegrate at the restrictive temperature, we aimed to stain endosomes with FM4-64. However, loss of Yup1 at the restrictive temperature prevented uptake of the fluorescent dye to shuttling endosomes (supplementary material Fig. S4), showing that FM4-64 staining is not able to answer this question. Therefore, we used the small G protein Rab5a, which has been intensively studied as an endosomal marker in *U. maydis*, to label endosomes (Schuster et al., 2011a; Schuster et al., 2011b; Schuster et al., 2011c). Ectopic expression of an N-terminal fusion of eGFP to Rab5a in the genetic background of AB33 under control of the constitutively active P_{otef} promoter (Table 1) enabled detection of shuttling endosomes during filamentous growth (supplementary material Fig. S5). Investigation of the same allele in the genetic background of AB33yup1^{ts} revealed that prolonged growth at the restrictive temperature causes defects in endosomal movement, as indicated by the fact that the

Fig. 3. Kin3 and Rrm4 colocalise with FM4-64-positive endosomes. (**A**,**B**) Filaments of indicated AB33 derivatives stained with FM4-64 (inverted frames). Filamentous growth was elicited by changing the nitrogen source of the medium resulting in transcriptional activation of the bW2–bE1 heterodimer (see text for details). Kymographs of inverted movies recorded simultaneously with dual-colour detection (time and distance as indicated). Colocalisation of Kin3G^3 (A) or Rrm4G (B) with shuttling FM4-64-stained endosomes is indicated by arrowheads. (**C**–**E**) Filaments of indicated AB33 derivatives. Inverted frames of green and red fluorescence are shown detecting Rrm4G and FM4-64, respectively. Arrows indicate colocalisation of Rrm4G with immobile FM4-64-stained endosomes. Scale bars: 10 µm.

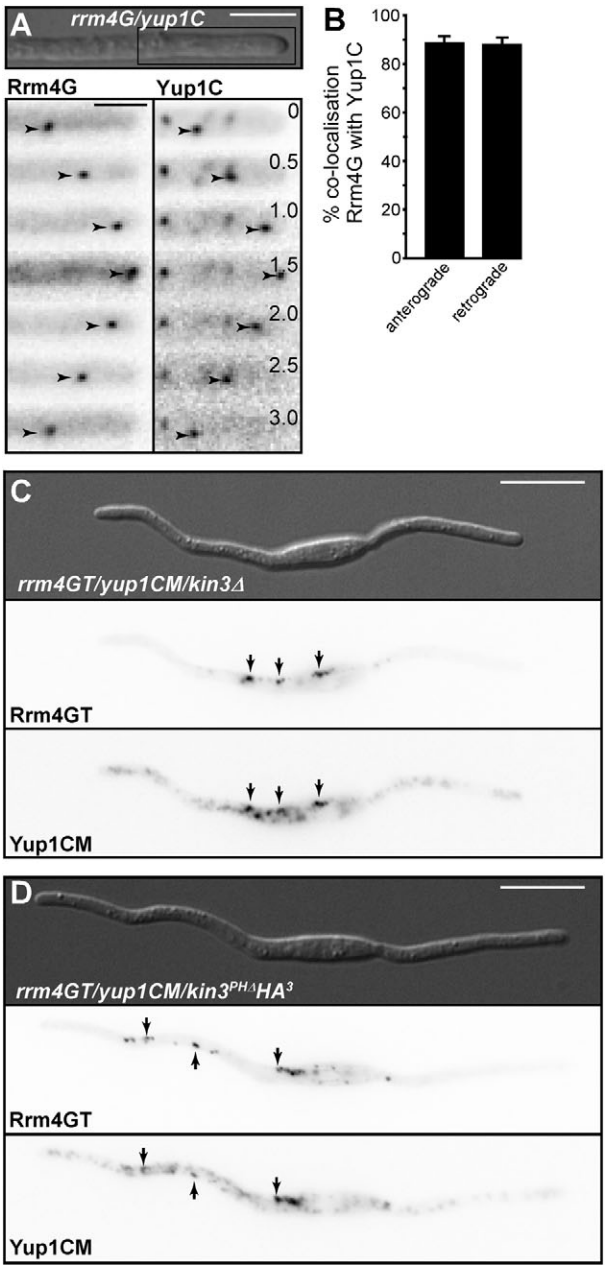

Fig. 4. Rrm4 associates with Yup1-positive endosomes independent of Kin3. (**A**) Filament tip of AB33rrm4G/yup1C. Filamentous growth was elicited by changing the nitrogen source of the medium resulting in transcriptional activation of the bW2–bE1 heterodimer (see text for details). Rectangle indicates region magnified below. Inverted frames are recorded with dual-colour detection and taken from supplementary material Movie 12. Images of green and red fluorescence were recorded simultaneously and are shown juxtaposed. Scale bars: 5 µm (top) and 2.5 µm (bottom). Arrowheads indicate moving units. Elapsed time is given in seconds. (**B**) Bar diagram showing the percentage of mobile Rrm4G signals that colocalise with Yup1C in the retrograde and anterograde direction (error bars, s.e.m.). (**C**,**D**) Filaments of AB33 derivatives as indicated. Inverted frames of green and red fluorescence (dual-colour mode) are shown detecting Rrm4GT and Yup1CM, respectively. Arrows indicate colocalisation of Rrm4GT with immobile Yup1-positive endosomes. Scale bars: 10 µm.

amount and the processivity of shuttling Rab5a-positive endosomes decreases (supplementary material Fig. S5). Thus, loss of Yup1 function does not simply cause the detachment of Rrm4-containing mRNPs, but has a profound influence on membrane trafficking at the level of endocytosis and endosome shuttling. Therefore, we conclude that microtubule-dependent shuttling of functional Yup1- and Rab5a-positive endosomes is essential for Rrm4 transport through the filament.

Discussion

Despite considerable efforts and substantial progress, the precise mechanisms of microtubule-dependent mRNP transport in eukaryotes are still elusive (Holt and Bullock, 2009; Meignin and Davis, 2010). In particular, the exact motor composition, as well as the involvement of membrane trafficking, are not clear. In this study, we identify the motor combination that mediates microtubule-dependent mRNP shuttling and provide in vivo evidence for the co-transport of mRNPs and endosomes along microtubules. An important strength of our experimental system is the ability to generate strains by homologous recombination. Therefore, the dynamics and subcellular localisation of mRNP components, as well as molecular motors, can be recorded at native expression levels.

Kinesin-3 and split dynein mediate shuttling of mRNPs in *U. maydis*

In many eukaryotic model systems, molecular motors mediate active shuttling of mRNPs along microtubules. This can be achieved by a single unidirectional motor along antipolar microtubules or by two motors with opposite directionality along polarised microtubule arrays. The motor repertoire of mRNP transport has been studied to varying extents in different systems. In mammalian neurons, biochemical purification of Staufen-containing mRNPs revealed the presence of conventional kinesin (Mallardo et al., 2003). In oocytes of *Xenopus laevis* kinesin-1-type and kinesin-3-type motors coordinate mRNP transport to the vegetal cortex on subpopulations of microtubules (Messitt et al., 2008). In oocytes of *D. melanogaster*, *oskar* mRNPs move bidirectionally along a weakly polarised microtubule cytoskeleton, and conventional kinesin is responsible for most of the transport (Zimyanin et al., 2008). Furthermore, in syncytial blastoderm embryos of *D. melanogaster*, the RNA-binding protein Egalitarian interacts with the dynein light chain with bicaudal-D and forms a functional transport complex in concert with dynactin and the dynein heavy chain (Dienstbier et al., 2009). However, in none of these systems has the whole motor composition been identified to completely explain the shuttling mechanism of mRNPs during microtubule-dependent transport.

In this study, we addressed the motor composition of Rrm4-containing mRNPs in *U. maydis* filaments and uncovered the concerted action of the kinesin Kin3 and the split dynein Dyn1–Dyn2 in mediating mRNP shuttling along microtubules. These findings were based on previous work studying the role of molecular motors in microtubule-dependent transport of endosomes in *U. maydis* (Steinberg, 2007b). Microtubules form two to four bundles that span the entire length of the filament. Within these bundles, individual microtubules are arranged in an antipolar array. At the poles, the microtubules no longer overlap and thus form a short unipolar region with plus ends facing towards the poles. Consequently, the region close to the poles is devoid of minus ends (Schuster et al., 2011c). Study of endosomal transport revealed that two to five Kin3 motors mediate plus-end-directed and highly processive movement throughout the whole filament (Schuster et al., 2011a; Schuster

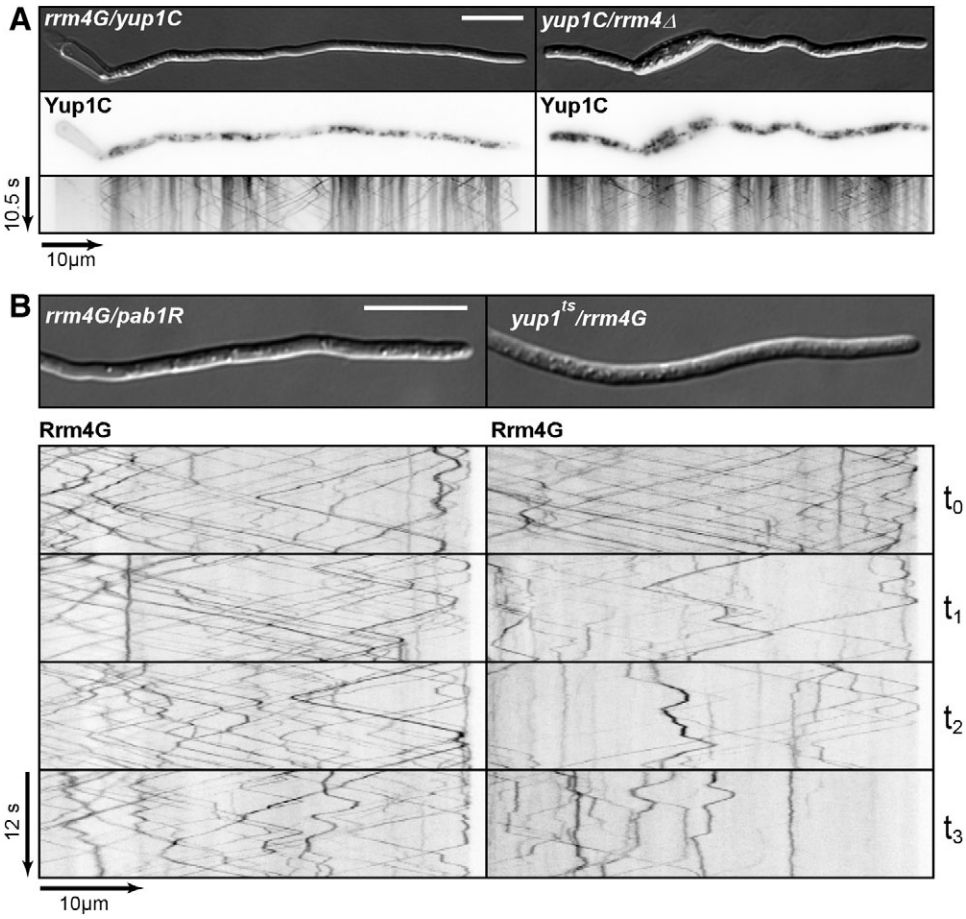

Fig. 5. Functional Yup1-positive vesicles are essential for mRNP transport. (**A**) Filaments of AB33rrm4G/yup1C and AB33rrm4Δ/yup1C on the left and right, respectively. Filamentous growth was elicited by changing the nitrogen source of the medium resulting in transcriptional activation of the bW2–bE1 heterodimer (see text for details). Inverted frames detecting Yup1C fluorescence and corresponding kymographs are shown (time and distance is given on the left). (**B**) Filaments of AB33rrm4G/pab1R and AB33rrm4G/yup1^{ts} on the left and right, respectively. Kymographs (time and distance is given on the left) of inverted movies detecting Rrm4G fluorescence at different time intervals at restrictive temperature are shown (t_0 to t_3=0, 30, 53 and 60 minutes, respectively). Note that the frames of the respective kymographs were recorded from the same filament and that both filaments were analysed in the same field of view to guarantee equal temperature conditions. Strains could be differentiated by the red fluorescence signal of Pab1R in AB33rrm4G/pab1R. Scale bars: 10 µm.

et al., 2011c). Split dynein Dyn1–Dyn2 is responsible for minus-end-directed movement. Because microtubule bundles are unipolar at the poles, Dyn1–Dyn2 is particularly important for the transport from the poles towards the zone of antipolar microtubules. In this region, endosomes can be transported by either split dynein or Kin3 (Schuster et al., 2011b; Schuster et al., 2011c). Earlier work demonstrated that conventional kinesin Kin1 in fruit flies and filamentous fungi is important to transport dynein back to the plus ends of microtubules (Januschke et al., 2002; Zhang et al., 2003; Lenz et al., 2006). This explains the observation that Rrm4-containing mRNPs accumulate at the poles in the absence of Kin1 (Becht et al., 2006) (this study).

Using a previously characterised temperature-sensitive allele of *dyn2* (Wedlich-Söldner et al., 2002b), we were able to demonstrate that the minus-end-directed transport of mRNPs in infectious filaments is mediated by dynein. Consistently, Dyn2 colocalised mainly with minus-end-directed Rrm4-containing mRNPs at the poles. Because microtubules are clearly unipolarly organised at the growing poles, our study focused on this region of the filament (Schuster et al., 2011c). Analysis of Kin3 revealed that this motor is essential for transport of mRNPs towards the plus ends of microtubules. Kin3 and Rrm4 also colocalise on retrograde moving units, indicating that the motor is recycled and that no independent backward transport of Kin3 towards minus ends of microtubules by an additional molecular motor is needed. Again, this becomes particularly evident in the unipolarly arranged region at the hyphal poles. The idea of Kin3 recycling is also supported by our observation that the protein variant lacking its PH domain is as stable as full length Kin3. By contrast, UNC-104 from *Caenorhabditis elegans* is degraded in the absence of vesicle cargo, suggesting that in this model system the motor is not reused after cargo deposition (Kumar et al., 2010). In summary, plus-end-directed transport along microtubules in *U. maydis* is mediated by Kin3 that does not dissociate from the transport unit, whereas split Dyn1–Dyn2 mediates minus-end-directed movement and is then independently returned to the microtubule plus ends by the action of Kin1. Thus, the combination of these three motors mediates bidirectional long-distance transport of mRNPs along microtubules.

Active co-transport of mRNPs and endosomes along microtubules

The contribution of membrane trafficking to mRNP transport is presently not clear. Even in the best-studied actin-dependent system, *ASH1* mRNA transport in *Saccharomyces cerevisiae*, controversial models are reported for the transport mechanisms. The traditional model describes the formation of a ‘locasome’, consisting of cargo mRNAs containing mRNA zip codes that are recognised by the concerted action of two unconventional RNA-binding proteins, She2p and She3p (Böhl et al., 2000; Müller et al., 2011). The resulting mRNP complex is transported by the molecular motor Myo4p along actin cables to the daughter cell (Müller et al., 2007; Paquin and Chartrand, 2008). This model was recently challenged by demonstrating a coordination of endoplasmic reticulum (ER) transport with cargo mRNA

movement, suggesting a close link between mRNP and membrane trafficking (Schmid et al., 2006; Gerst, 2008).

Microtubule-dependent shuttling of mRNPs is crucial for a variety of different cellular events such as developmental and neuronal processes (Martin and Ephrussi, 2009; Meignin and Davis, 2010; Doyle and Kiebler, 2011). Among the best-studied examples is transport of pair-rule transcripts during embryogenesis. Egl recognizes mRNA zip codes and associates with Bic-D, which interacts with dynein and apparently increases motor processivity (Dienstbier et al., 2009). Intriguingly, Bic-D is also important for vesicle transport in neurons. However, this is an Egl-independent process. Thus, at least in neurons, mRNA transport and vesicle transport seem to be independent (Li et al., 2010).

In oocytes, it was shown that shuttling occurs along a weakly polarised cytoskeleton involving the RNA-binding protein Staufen and Kin1 (Zimyanin et al., 2008). However, the orientation of the microtubule arrays and the potential role of dynein are not solved. Interestingly, a potential connection to membrane trafficking has also been described in this system. The endosomal marker Rab11, for example, is important for localisation of *oskar* mRNA and this small G protein accumulates similar to the mRNA target at the posterior poles of oocytes (Dollar et al., 2002; Cohen, 2005). Additional hints for a connection to membrane trafficking are the observation that mutants in components of ESCRT-II (endosomal sorting complex required for transport) abolish a Staufen-dependent step in the localisation of *bicoid* mRNA (Irion and St Johnston, 2007), and that genomic RNAs of mammalian retroviruses are transported on recycling endosomes in mammals (Basyuk et al., 2003; Molle et al., 2009).

In this study, we provide the first direct in vivo evidence for the co-transport of mRNPs and endosomes. As mentioned above, Rrm4-containing mRNPs rely on the same motor repertoire as shuttling endosomes suggesting their co-transport (Lenz et al., 2006; Steinberg, 2007a; Schuster et al., 2011c; Schuster et al., 2011a). This was verified by in vivo studies demonstrating that functional Kin3 or its lipid-binding PH domain are crucial for mRNP transport and that Rrm4 colocalises with the lipophilic dye FM4-64, as well as the endosomal marker Yup1.

In theory, the endosome and mRNP co-transport could be mediated by at least two different mechanisms that might both include the action of adapter proteins: (1) molecular motors contain two distinct interaction domains, one for Rrm4 binding and one for the interaction with endosomes such as the lipid-binding PH domain or (2) Rrm4 binds to endosomes and transport is mediated, for example, through the PH domain of Kin3. An example for such an adaptor is Bic-D from *D. melanogaster*, which interacts with dynein and plays a role in both vesicle and mRNP transport (Dienstbier and Li, 2009; Li et al., 2010). In *U. maydis*, direct binding to dynein as the sole mode of mRNP shuttling can be excluded, because dynein is absent from most of the anterograde moving Rrm4 units. Direct binding to kinesin Kin3 could be possible, because it has been reported that conventional kinesin appears to interact directly with the RNA-binding protein FMRP during dendritic mRNA transport (Dictenberg et al., 2008). However, we favour the hypothesis that Rrm4 binds to endosomes independent of Kin3. This is based on our findings that Rrm4 colocalises with Yup1 in the absence of Kin3 or in strains expressing Kin3 without lipid-binding PH domain. It remains to be seen whether Rrm4 needs an adaptor or can directly bind for example to specific endosomal lipids. Our analysis of the functional relationship of Rrm4 and endosome transport revealed that whereas endosome transport does not need mRNPs, mRNP transport depends on functional Rab5a-positive endosomes. Thus, we demonstrate that long-distance transport of Rrm4-containing mRNPs is functionally linked to endosome transport.

Microtubule-dependent transport is crucial in determining the axis of polarity in infectious filaments of *U. maydis*. Inhibition of polymerisation of microtubules with benomyl results in the formation of filaments that are shorter, grow bipolarly and are impaired in the insertion of retraction septa (Fuchs et al., 2005). The same is true in the absence of the plus-end-directed molecular motors Kin1 and Kin3 (Becht et al., 2005; Schuchardt et al., 2005) and when interfering with the split dynein function (this study). Importantly, the axis of polarity and the formation of retraction septa are also disturbed in Rrm4 mutants that are affected in RNA binding, resulting in transport of endosomes without Pab1-associated mRNAs (König et al., 2009). Because loss of Rrm4 does not interfere with endosome movement, these effects are likely to reflect the functional importance of mRNP transport during polar growth.

In conclusion, we present strong evidence for a novel and unexpected link between endosome and mRNP transport. This adds yet another function to trafficking endosomes and is consistent with current views that these vesicular carriers function as multi-purpose platforms (Gould and Lippincott-Schwartz, 2009). Elucidation of further mechanistic details will be crucial to advance our understanding of mRNA transport and its function in spatio-temporal gene expression.

Materials and Methods

Strains and growth conditions

E. coli K-12 derivatives DH5α and Top10 (Invitrogen, Darmstadt, Germany) were used for cloning purposes. Transformation and cultivation were performed using standard techniques. Growth conditions for *U. maydis* strains and source of antibiotics were previously described (Brachmann et al., 2004). Strains were constructed by the transformation of progenitor strains with linearised plasmids (Table 1; supplementary material Table S1). All homologous integration events were verified by Southern blot analysis (Brachmann et al., 2004). For strains AB33P_{otef}yup1C, AB33P_{otef}yup1CM and AB33P_{otef}rab5aG respective plasmid vectors pP_{otef}yup1C, pP_{otef}yup1CM or pP_{otef}rab5aG were linearised with Ssp1 and targeted to the ip^S locus of AB33 (Loubradou et al., 2001). In the case of strain AB5, vector pAB33 (Brachmann et al., 2001) linearised with SspI was transformed into FB1. Homologous integration and the functionality of both *nar1* promoters driving *bW2* and *bE1* expression was verified by Southern and northern analysis, respectively.

Filamentous growth of AB33 and AB5 variants was induced by shifting 20 or 50 ml of exponentially growing cells (OD_{600}=0.4–0.5) from complete medium (CM) to nitrate minimal medium (NM) each supplemented with 1% glucose (glc). Cells were incubated at 28℃ shaking at 200 r.p.m. for 4–8 hours before microscopy. The temperature-sensitive strain AB5dyn2^{ts}/rrm4G/pab1R was induced for 15 hours at permissive (18℃) and restrictive (28℃) temperatures. For verification of temperature sensitivity on plates, cells were grown to an OD_{600} of 1. Tenfold dilutions were spotted on CM agar and incubated at either 18 or 30℃. Analysis of temperature-sensitive growth was performed as indicated in the legend of supplementary material Fig. S2.

Plasmids and plasmid construction

Standard molecular techniques and strain generation methods for *U. maydis* were followed. Plasmids pCRII-Topo (Invitrogen) and pBluescriptSKII (Stratagene) were used as cloning vehicles. Genomic DNA of wild-type strain UM521 (*a1b1*) was used as a template for PCR amplifications unless otherwise noted. All constructs were confirmed by sequencing. Detailed information is given in supplementary material Tables S2 and S3 and plasmid sequences are available upon request.

Chemicals and media

Chemicals and media used in this study were purchased from Difco (Augsburg, Germany), Sigma (Steinheim, Germany), Merck (Darmstadt, Germany), Baker (Griesheim, Germany), VWR (Darmstadt, Germany) and Roth (Karlsruhe, Germany). Restriction enzymes were obtained from NEB (Frankfurt, Germany), Phusion-Polymerase from Finnzymes (Schwerte, Germany) and T4-Ligase from Roche (Mannheim, Germany).

Microscopy, image processing, quantitative analysis and FM4-64 staining

Microscopy was performed on the following wide-field microscopes from Visitron Systems (Munich, Germany): (1) Zeiss (Oberkochen, Germany) Axiovert 200M equipped with a charge-coupled device camera (CCD; Photometrics CoolSNAP HQ, Tucson, AZ) and objective lenses Plan Neofluar (40×, NA 0.75) and Plan Apochromat (63× and 100×, NA 1.4). (2) Zeiss Axio Observer.Z1 equipped with a CCD camera (Photometrics CoolSNAP HQ2) and objective lenses Plan Neofluar (40×, NA 1.3), Plan Apochromat (63× and 100×, NA 1.4) and α-Plan Apochromat (100×, NA 1.46). (3) Zeiss Axio Imager.M1 equipped with a Spot Pursuit CCD camera (Diagnostic Instruments, Sterling Heights, MI) and objective lenses Plan Neofluar (40× and 100×, NA 1.3; 63×, NA 1.25).

Excitation of fluorescently labelled proteins was carried out using an HBO 103 mercury lamp or HXP metal halide lamps (LEj, Jena, Germany) in combination with filter sets for GFP (ET470/40BP, ET495LP, ET525/50BP) and RFP and mCherry (ET560/40BP, ET585LP, ET630/75BP; Chroma, Bellow Falls, VT). For detection of weak signals we used laser-based epifluorescence microscopy. A VS-LMS4 Laser-Merge-System (Visitron Systems) combines solid state lasers for the excitation of GFP (488 nm/50 mW) and RFP or mCherry (561 nm/50 mW).

Colocalisation studies of dynamic processes were carried out with a two-channel imager (DV2, Photometrics) that permits the simultaneous detection of GFP and RFP or mCherry. A dichroic beamsplitter and an excitation filter designed for GFP and mCherry (GFP/mCherry; Chroma) were used to simultaneously excite the respective fluorophores. A second dichroic beamsplitter (dcxr565) within the dual-view device split the fluorescent signals into the respective colours that were separately filtered with emission filters (GFP ET520/40; RFP/mCherry ET632/60) before simultaneous imaging on different regions of the CCD chip.

To observe RrmG in strain AB5dyn2^{ts}/rrm4G a 472 nm LED (CoolLED, precisExcite, Andover, UK) was used to reduce photobleaching to a minimum. All parts of the microscope systems were controlled by the software package MetaMorph (Molecular Devices, version 6 and 7, Sunnyvale, CA), which was also used for image processing including the adjustment of brightness and contrast, as well as the generation of kymographs.

For the quantification of colocalising proteins on moving vesicles, a segment of 10 µm from the apical pole in each filament was defined. Rrm4-containing units were counted and tested for the presence of Dyn2, Kin3 or Yup1. In each case, three independent experiments were carried out with 10 (Dyn2), 8–10 (Kin3) and 5 (Yup1) filaments per experiment. The average amount of colocalising proteins and the s.e. were determined.

For FM4-64 staining 1 ml of filament suspension was labelled in 0.8 µM FM4-64 (Invitrogen; for AB5dyn2^{ts}/rrm4G 4 µM FM4-64 was used). After 30–60 seconds of incubation at room temperature, samples were subjected to microscopic analysis. For AB33yup1^{ts}/rrm4G, filaments were also incubated at the restrictive temperature (supplementary material Fig. S4).

Microscopic analysis of temperature-sensitive mutants

For analysis of AB33yup1^{ts}/rrm4G, the temperature in the sample was adjusted by pumping water from a water bath (Huber, Offenburg, Germany) controlled by Metamorph software through a flexible tube connected to a metal ring plugged onto the objective. Thereby, heat is transferred through the immersion oil to the sample. Because the exact temperature in the sample cannot be determined, the temperature-sensitive strain AB33yup1^{ts}/rrm4G and control strain AB33rrm4G/pab1R were mixed in equal amounts. In initial experiments, a temperature of 48.5℃ in the water bath was determined to have an impact on Rrm4G movement in AB33yup1^{ts}/rrm4G but not in AB33rrm4G/pab1R. Immediately after identifying regions containing both strains in the field of vision, the observation of Rrm4G movement was started. Four subsequent movies were recorded at time points 0, 30 minutes, 53 minutes and 60 minutes. Each movie is 12 seconds long (80 frames, 150 mseconds). The resulting movies were converted to kymographs.

For experiments with AB33yup1^{ts}/rab5aG (supplementary material Fig. S5) a water bath temperature of 45℃ was determined to confer restrictive conditions at the microscopic sample. This temperature had an effect on Rab5aG-positive endosomes in *yup1^{ts}* mutants after prolonged exposure but had no effect on control strain AB33rab5aG expressing endogenous Yup1. Four subsequent movies were recorded at time points 0, 12 minutes, 46 minutes and 92 minutes. Each movie is 15 seconds in length (100 frames, 150 mseconds). The resulting movies were converted to kymographs. The lower temperature (45℃ versus 48.5℃, see above) probably reflects a minor defect caused by expression of Rab5aG.

The same experimental set-up was used to analyse AB5dyn2^{ts}/rrm4G. Filaments were observed microscopically either at permissive temperature (21℃) or at restrictive temperature (water bath set to 45℃). Single movies with 500 frames of 300 mseconds were recorded and converted to kymographs.

Protein preparation and western blot analysis

Filaments were harvested by centrifugation (10,000 ***g***, 5 minutes) and resuspended in 2 ml UmVIB buffer (20 mM HEPES-NaOH, pH 7.4, 400 mM Sorbitol, 150 mM NaCl, 5 mM $MgCl_2$, 1 mM EDTA, 1 mM DTT). Cells were frozen in liquid nitrogen and ground for 15 minutes in a pebble mill. The protein concentration was determined by Bradford assay (Bio-Rad, Munich, Germany). Protein samples were resolved by 8% SDS-PAGE and transferred to a PVDF membrane (GE Healthcare, Munich, Germany) by semi-dry blotting [5 µg of protein were loaded for western blot analysis with anti-GFP (Roche, Freiburg, Germany) and anti-Tub (Sigma) antibodies]. A mouse IgG HRP conjugate (H+L; Promega, Madison, WI) was used as a secondary antibody. Activity was detected using the ECL plus western blotting detection system (GE Healthcare).

Acknowledgements

We acknowledge Kathi Zarnack as well as lab members for valuable discussion and critical reading of the manuscript. We are grateful to Gero Steinberg for insights on microtubule-dependent transport and for constructs pDyn2G^3-HygR, pKin3-kohyg-RWS74 and the *dyn2^{ts}* allele as well as strain AB33yup1^{ts}. Kai Schink and Michael Bölker provided construct pP$_{otef}$Yup1C-CbxR and William K. Holloman plasmid pUCLII Otef-Neo carrying the geneticin resistance gene. Kathi Zarnack, Philipp Müller and Emir Islamovic constructed plasmids pMF5-4h, pMF5-9h and pMF5-1c, respectively. Special thanks to Petra Happel and Ute Gengenbacher for excellent technical assistance and Regine Kahmann from the Max Planck Institute for Terrestrial Microbiology for support on microscopy infrastructure and laboratory equipment.

Funding

The work was supported by grants from the Deutsche Forschungsgemeinschaft [grant number FE 448/5-1] to M.F. as part of the German/Mexican research group FOR1334.

Supplementary material available online at
http://jcs.biologists.org/lookup/suppl/doi:10.1242/jcs.101212/-/DC1

References

Banuett, F. and Herskowitz, I. (1989). Different *a* alleles of *Ustilago maydis* are necessary for maintenance of filamentous growth but not for meiosis. *Proc. Natl. Acad. Sci. USA* **86**, 5878-5882.

Basyuk, E., Galli, T., Mougel, M., Blanchard, J. M., Sitbon, M. and Bertrand, E. (2003). Retroviral genomic RNAs are transported to the plasma membrane by endosomal vesicles. *Dev. Cell* **5**, 161-174.

Becht, P., Vollmeister, E. and Feldbrügge, M. (2005). Role for RNA-binding proteins implicated in pathogenic development of *Ustilago maydis*. *Eukaryot. Cell* **4**, 121-133.

Becht, P., König, J. and Feldbrügge, M. (2006). The RNA-binding protein Rrm4 is essential for polarity in *Ustilago maydis* and shuttles along microtubules. *J. Cell Sci.* **119**, 4964-4973.

Böhl, F., Kruse, C., Frank, A., Ferring, D. and Jansen, R. P. (2000). She2p, a novel RNA-binding protein tethers *ASH1* mRNA to the Myo4p myosin motor via She3p. *EMBO J.* **19**, 5514-5524.

Brachmann, A., Weinzierl, G., Kämper, J. and Kahmann, R. (2001). Identification of genes in the bW/bE regulatory cascade in *Ustilago maydis*. *Mol. Microbiol.* **42**, 1047-1063.

Brachmann, A., König, J., Julius, C. and Feldbrügge, M. (2004). A reverse genetic approach for generating gene replacement mutants in *Ustilago maydis*. *Mol. Genet. Genomics* **272**, 216-226.

Brefort, T., Doehlemann, G., Mendoza-Mendoza, A., Reissmann, S., Djamei, A. and Kahmann, R. (2009). *Ustilago maydis* as a Pathogen. *Annu. Rev. Phytopathol.* **47**, 423-445.

Bullock, S. L., Nicol, A., Gross, S. P. and Zicha, D. (2006). Guidance of bidirectional motor complexes by mRNA cargoes through control of dynein number and activity. *Curr. Biol.* **16**, 1447-1452.

Cohen, R. S. (2005). The role of membranes and membrane trafficking in RNA localization. *Biol. Cell* **97**, 5-18.

Delanoue, R. and Davis, I. (2005). Dynein anchors its mRNA cargo after apical transport in the *Drosophila* blastoderm embryo. *Cell* **122**, 97-106.

Delanoue, R., Herpers, B., Soetaert, J., Davis, I. and Rabouille, C. (2007). *Drosophila* Squid/hnRNP helps Dynein switch from a *gurken* mRNA transport motor to an ultrastructural static anchor in sponge bodies. *Dev. Cell* **13**, 523-538.

Dictenberg, J. B., Swanger, S. A., Antar, L. N., Singer, R. H. and Bassell, G. J. (2008). A direct role for FMRP in activity-dependent dendritic mRNA transport links filopodial-spine morphogenesis to fragile X syndrome. *Dev. Cell* **14**, 926-939.

Dienstbier, M. and Li, X. (2009). Bicaudal-D and its role in cargo sorting by microtubule-based motors. *Biochem. Soc. Trans.* **37**, 1066-1071.

Dienstbier, M., Boehl, F., Li, X. and Bullock, S. L. (2009). Egalitarian is a selective RNA-binding protein linking mRNA localization signals to the dynein motor. *Genes Dev.* **23**, 1546-1558.

Dollar, G., Struckhoff, E., Michaud, J. and Cohen, R. S. (2002). Rab11 polarization of the *Drosophila* oocyte: a novel link between membrane trafficking, microtubule organization, and oskar mRNA localization and translation. *Development* **129**, 517-526.

Doyle, M. and Kiebler, M. A. (2011). Mechanisms of dendritic mRNA transport and its role in synaptic tagging. *EMBO J.* **30**, 3540-3552.

Feldbrügge, M., Zarnack, K., Vollmeister, E., Baumann, S., Koepke, J., König, J., Münsterkötter, M. and Mannhaupt, G. (2008). The posttranscriptional machinery of *Ustilago maydis*. *Fungal Genet. Biol.* **45 Suppl. 1**, S40-S46.

Fuchs, U., Manns, I. and Steinberg, G. (2005). Microtubules are dispensable for the initial pathogenic development but required for long-distance hyphal growth in the corn smut fungus *Ustilago maydis*. *Mol. Biol. Cell* **16**, 2746-2758.

Fuchs, U., Hause, G., Schuchardt, I. and Steinberg, G. (2006). Endocytosis is essential for pathogenic development in the corn smut fungus *Ustilago maydis*. *Plant Cell* **18**, 2066-2081.

Gennerich, A. and Vale, R. D. (2009). Walking the walk: how kinesin and dynein coordinate their steps. *Curr. Opin. Cell Biol.* **21**, 59-67.

Gerst, J. E. (2008). Message on the web: mRNA and ER co-trafficking. *Trends Cell Biol.* **18**, 68-76.

Gould, G. W. and Lippincott-Schwartz, J. (2009). New roles for endosomes: from vesicular carriers to multi-purpose platforms. *Nat. Rev. Mol. Cell Biol.* **10**, 287-292.

Hogan, D. J., Riordan, D. P., Gerber, A. P., Herschlag, D. and Brown, P. O. (2008). Diverse RNA-binding proteins interact with functionally related sets of RNAs, suggesting an extensive regulatory system. *PLoS Biol.* **6**, e255.

Holt, C. E. and Bullock, S. L. (2009). Subcellular mRNA localization in animal cells and why it matters. *Science* **326**, 1212-1216.

Irion, U. and St Johnston, D. (2007). *bicoid* RNA localization requires specific binding of an endosomal sorting complex. *Nature* **445**, 554-558.

Januschke, J., Gervais, L., Dass, S., Kaltschmidt, J. A., Lopez-Schier, H., St Johnston, D., Brand, A. H., Roth, S. and Guichet, A. (2002). Polar transport in the *Drosophila* oocyte requires Dynein and Kinesin I cooperation. *Curr. Biol.* **12**, 1971-1981.

Jenny, A., Hachet, O., Závorszky, P., Cyrklaff, A., Weston, M. D., Johnston, D. S., Erdélyi, M. and Ephrussi, A. (2006). A translation-independent role of oskar RNA in early *Drosophila* oogenesis. *Development* **133**, 2827-2833.

Kämper, J., Reichmann, M., Romeis, T., Bölker, M. and Kahmann, R. (1995). Multiallelic recognition: nonself-dependent dimerization of the bE and bW homeodomain proteins in *Ustilago maydis*. *Cell* **81**, 73-83.

Kämper, J., Kahmann, R., Bölker, M., Ma, L. J., Brefort, T., Saville, B. J., Banuett, F., Kronstad, J. W., Gold, S. E., Müller, O. et al. (2006). Insights from the genome of the biotrophic fungal plant pathogen *Ustilago maydis*. *Nature* **444**, 97-101.

King, M. L., Messitt, T. J. and Mowry, K. L. (2005). Putting RNAs in the right place at the right time: RNA localization in the frog oocyte. *Biol. Cell* **97**, 19-33.

Klopfenstein, D. R. and Vale, R. D. (2004). The lipid binding pleckstrin homology domain in UNC-104 kinesin is necessary for synaptic vesicle transport in *Caenorhabditis elegans*. *Mol. Biol. Cell* **15**, 3729-3739.

Klopfenstein, D. R., Tomishige, M., Stuurman, N. and Vale, R. D. (2002). Role of phosphatidylinositol(4,5)bisphosphate organization in membrane transport by the Unc104 kinesin motor. *Cell* **109**, 347-358.

Koepke, J., Kaffarnik, F., Haag, C., Zarnack, K., Luscombe, N. M., König, J., Ule, J., Kellner, R., Begerow, D. and Feldbrügge, M. (2011). The RNA-binding protein Rrm4 is essential for efficient secretion of endochitinase Cts1. *Mol. Cell. Proteomics* **10**, M111.011213 1-15.

König, J., Baumann, S., Koepke, J., Pohlmann, T., Zarnack, K. and Feldbrügge, M. (2009). The fungal RNA-binding protein Rrm4 mediates long-distance transport of *ubi1* and *rho3* mRNAs. *EMBO J.* **28**, 1855-1866.

Kozlov, G., Ménade, M., Rosenauer, A., Nguyen, L. and Gehring, K. (2010). Molecular determinants of PAM2 recognition by the MLLE domain of poly(A)-binding protein. *J. Mol. Biol.* **397**, 397-407.

Kozlov, G., Trempe, J. F., Khaleghpour, K., Kahvejian, A., Ekiel, I. and Gehring, K. (2001). Structure and function of the C-terminal PABC domain of human poly(A)-binding protein. *Proc. Natl. Acad. Sci. USA* **98**, 4409-4413.

Kumar, J., Choudhary, B. C., Metpally, R., Zheng, Q., Nonet, M. L., Ramanathan, S., Klopfenstein, D. R. and Koushika, S. P. (2010). The *Caenorhabditis elegans* Kinesin-3 motor UNC-104/KIF1A is degraded upon loss of specific binding to cargo. *PLoS Genet.* **6**, e1001200.

Lehmler, C., Steinberg, G., Snetselaar, K. M., Schliwa, M., Kahmann, R. and Bölker, M. (1997). Identification of a motor protein required for filamentous growth in *Ustilago maydis*. *EMBO J.* **16**, 3464-3473.

Lenz, J. H., Schuchardt, I., Straube, A. and Steinberg, G. (2006). A dynein loading zone for retrograde endosome motility at microtubule plus-ends. *EMBO J.* **25**, 2275-2286.

Letunic, I., Doerks, T. and Bork, P. (2009). SMART 6: recent updates and new developments. *Nucleic Acids Res.* **37 Database issue**, D229-D232.

Li, R. and Gundersen, G. G. (2008). Beyond polymer polarity: how the cytoskeleton builds a polarized cell. *Nat. Rev. Mol. Cell Biol.* **9**, 860-873.

Li, X., Kuromi, H., Briggs, L., Green, D. B., Rocha, J. J., Sweeney, S. T. and Bullock, S. L. (2010). Bicaudal-D binds clathrin heavy chain to promote its transport and augments synaptic vesicle recycling. *EMBO J.* **29**, 992-1006.

Loubradou, G., Brachmann, A., Feldbrügge, M. and Kahmann, R. (2001). A homologue of the transcriptional repressor Ssn6p antagonizes cAMP signalling in Ustilago maydis. *Mol. Microbiol.* **40**, 719-730.

Mallardo, M., Deitinghoff, A., Müller, J., Goetze, B., Macchi, P., Peters, C. and Kiebler, M. A. (2003). Isolation and characterization of Staufen-containing ribonucleoprotein particles from rat brain. *Proc. Natl. Acad. Sci. USA* **100**, 2100-2105.

Martin, K. C. and Ephrussi, A. (2009). mRNA localization: gene expression in the spatial dimension. *Cell* **136**, 719-730.

Meignin, C. and Davis, I. (2010). Transmitting the message: intracellular mRNA localization. *Curr. Opin. Cell Biol.* **22**, 112-119.

Messitt, T. J., Gagnon, J. A., Kreiling, J. A., Pratt, C. A., Yoon, Y. J. and Mowry, K. L. (2008). Multiple kinesin motors coordinate cytoplasmic RNA transport on a subpopulation of microtubules in *Xenopus* oocytes. *Dev. Cell* **15**, 426-436.

Molle, D., Segura-Morales, C., Camus, G., Berlioz-Torrent, C., Kjems, J., Basyuk, E. and Bertrand, E. (2009). Endosomal trafficking of HIV-1 gag and genomic RNAs regulates viral egress. *J. Biol. Chem.* **284**, 19727-19743.

Müller, M., Heuck, A. and Niessing, D. (2007). Directional mRNA transport in eukaryotes: lessons from yeast. *Cell. Mol. Life Sci.* **64**, 171-180.

Müller, M., Heym, R. G., Mayer, A., Kramer, K., Schmid, M., Cramer, P., Urlaub, H., Jansen, R. P. and Niessing, D. (2011). A cytoplasmic complex mediates specific mRNA recognition and localization in yeast. *PLoS Biol.* **9**, e1000611.

Niman, H. L., Houghten, R. A., Walker, L. E., Reisfeld, R. A., Wilson, I. A., Hogle, J. M. and Lerner, R. A. (1983). Generation of protein-reactive antibodies by short peptides is an event of high frequency: implications for the structural basis of immune recognition. *Proc. Natl. Acad. Sci. USA* **80**, 4949-4953.

Palacios, I. M. (2007). How does an mRNA find its way? Intracellular localisation of transcripts. *Semin. Cell Dev. Biol.* **18**, 163-170.

Paquin, N. and Chartrand, P. (2008). Local regulation of mRNA translation: new insights from the bud. *Trends Cell Biol.* **18**, 105-111.

Schink, K. O. and Bölker, M. (2009). Coordination of cytokinesis and cell separation by endosomal targeting of a Cdc42-specific guanine nucleotide exchange factor in *Ustilago maydis*. *Mol. Biol. Cell* **20**, 1081-1088.

Schmid, M., Jaedicke, A., Du, T. G. and Jansen, R. P. (2006). Coordination of endoplasmic reticulum and mRNA localization to the yeast bud. *Curr. Biol.* **16**, 1538-1543.

Schuchardt, I., Assmann, D., Thines, E., Schuberth, C. and Steinberg, G. (2005). Myosin-V, Kinesin-1, and Kinesin-3 cooperate in hyphal growth of the fungus *Ustilago maydis*. *Mol. Biol. Cell* **16**, 5191-5201.

Schuster, M., Lipowsky, R., Assmann, M. A., Lenz, P. and Steinberg, G. (2011a). Transient binding of dynein controls bidirectional long-range motility of early endosomes. *Proc. Natl. Acad. Sci. USA* **108**, 3618-3623.

Schuster, M., Kilaru, S., Fink, G., Collemare, J., Roger, Y. and Steinberg, G. (2011b). Kinesin-3 and dynein cooperate in long-range retrograde endosome motility along a nonuniform microtubule array. *Mol. Biol. Cell* **22**, 3645-3657.

Schuster, M., Kilaru, S., Ashwin, P., Lin, C., Severs, N. J. and Steinberg, G. (2011c). Controlled and stochastic retention concentrates dynein at microtubule ends to keep endosomes on track. *EMBO J.* **30**, 652-664.

Shaner, N. C., Campbell, R. E., Steinbach, P. A., Giepmans, B. N., Palmer, A. E. and Tsien, R. Y. (2004). Improved monomeric red, orange and yellow fluorescent proteins derived from *Discosoma* sp. red fluorescent protein. *Nat. Biotechnol.* **22**, 1567-1572.

St Johnston, D. (2005). Moving messages: the intracellular localization of mRNAs. *Nat. Rev. Mol. Cell Biol.* **6**, 363-375.

Steinberg, G. (2007a). Hyphal growth: a tale of motors, lipids, and the Spitzenkörper. *Eukaryot. Cell* **6**, 351-360.

Steinberg, G. (2007b). On the move: endosomes in fungal growth and pathogenicity. *Nat. Rev. Microbiol.* **5**, 309-316.

Steinberg, G., Schliwa, M., Lehmler, C., Bölker, M., Kahmann, R. and McIntosh, J. R. (1998). Kinesin from the plant pathogenic fungus *Ustilago maydis* is involved in vacuole formation and cytoplasmic migration. *J. Cell Sci.* **111**, 2235-2246.

Straube, A., Brill, M., Oakley, B. R., Horio, T. and Steinberg, G. (2003). Microtubule organization requires cell cycle-dependent nucleation at dispersed cytoplasmic sites: polar and perinuclear microtubule organizing centers in the plant pathogen *Ustilago maydis*. *Mol. Biol. Cell* **14**, 642-657.

Straube, A., Enard, W., Berner, A., Wedlich-Söldner, R., Kahmann, R. and Steinberg, G. (2001). A split motor domain in a cytoplasmic dynein. *EMBO J.* **20**, 5091-5100.

Vida, T. A. and Emr, S. D. (1995). A new vital stain for visualizing vacuolar membrane dynamics and endocytosis in yeast. *J. Cell Biol.* **128**, 779-792.

Vollmeister, E. and Feldbrügge, M. (2010). Posttranscriptional control of growth and development in *Ustilago maydis*. *Curr. Opin. Microbiol.* **13**, 693-699.

Vollmeister, E., Schipper, K., Baumann, S., Haag, C., Pohlmann, T., Stock, J. and Feldbrügge, M. (2012). Fungal development of the plant pathogen *Ustilago maydis*. *FEMS Microbiol. Rev.* **36**, 59-77.

Wedlich-Söldner, R., Bölker, M., Kahmann, R. and Steinberg, G. (2000). A putative endosomal t-SNARE links exo- and endocytosis in the phytopathogenic fungus *Ustilago maydis*. *EMBO J.* **19**, 1974-1986.

Journal of Cell Science

Wedlich-Söldner, R., Schulz, I., Straube, A. and Steinberg, G. (2002a). Dynein supports motility of endoplasmic reticulum in the fungus *Ustilago maydis*. *Mol. Biol. Cell* **13**, 965-977.

Wedlich-Söldner, R., Straube, A., Friedrich, M. W. and Steinberg, G. (2002b). A balance of KIF1A-like kinesin and dynein organizes early endosomes in the fungus *Ustilago maydis*. *EMBO J.* **21**, 2946-2957.

Zarnack, K. and Feldbrügge, M. (2007). mRNA trafficking in fungi. *Mol. Genet. Genomics* **278**, 347-359.

Zarnack, K. and Feldbrügge, M. (2010). Microtubule-dependent mRNA transport in fungi. *Eukaryot. Cell* **9**, 982-990.

Zhang, J., Li, S., Fischer, R. and Xiang, X. (2003). Accumulation of cytoplasmic dynein and dynactin at microtubule plus ends in *Aspergillus nidulans* is kinesin dependent. *Mol. Biol. Cell* **14**, 1479-1488.

Zimyanin, V. L., Belaya, K., Pecreaux, J., Gilchrist, M. J., Clark, A., Davis, I. and St Johnston, D. (2008). *In vivo* imaging of *oskar* mRNA transport reveals the mechanism of posterior localization. *Cell* **134**, 843-853.